Evolution of the Adsorbed Water Layer Structure on Silicon Oxide at Room Temperature

David B. Asay and Seong H. Kim*

Department of Chemical Engineering, The Pennsylvania State University, University Park, Pennsylvania 16802

Received: June 7, 2005; In Final Form: July 7, 2005

The molecular configuration of water adsorbed on a hydrophilic silicon oxide surface at room temperature has been determined as a function of relative humidity using attenuated total reflection (ATR)−infrared spectroscopy. A completely hydrogen-bonded icelike network of water grows up to three layers as the relative humidity increases from 0 to 30%. In the relative humidity range of 30−60%, the liquid water structure starts appearing while the icelike structure continues growing to saturation. The total thickness of the adsorbed layer increases only one molecular layer in this humidity range. Above 60% relative humidity, the liquid water configuration grows on top of the icelike layer. This structural evolution indicates that the outermost layer of the adsorbed water molecules undergoes transitions in equilibrium behavior as humidity varies. These transitions determine the shape of the adsorption isotherm curve. The structural transitions of the outermost adsorbed layer are accompanied by interfacial energy changes and explain many phenomena observed only for water adsorption.

Introduction

Water adsorbs onto virtually all surfaces. As a consequence, interfacial water plays important roles in biology,[1] meteorology,[2] geology,[3] and nanotechnology. Water structure at an interface is key to discerning wetting phenomena.[4] Surface chemistry and the structure of water molecules adsorbed at the surface determine biological phenomena like bioadhesion.[1,5] In micro- and nanomaterial engineering, the control of interfacial chemistry is critical because the surface-to-volume ratio is significantly large and surface properties dominate material performance.[6] For example, water adsorbed on hydrophilic silicon oxide surfaces causes large changes in adhesion and friction in nanoscale contacts.[7−9] Silicon oxide is abundant in nature and is important in semiconductors, cements,[10] and geology.[3] This paper shows how the molecular configuration of water molecules at the interface of the clean silicon oxide surface evolves as a function of relative humidity at room temperature.

The configuration of adsorbed water molecules has been studied extensively in ultrahigh vacuum conditions at cryogenic temperatures.[11−12] The knowledge obtained from these studies is useful in understanding water chemistry in the upper atmosphere or in space. However, it cannot be extrapolated to elucidate surface chemistry occurring at ambient conditions. There have been many spectroscopic, microscopic, and theoretical studies of thin-film interactions and molecular configurations at the bulk water/substrate interface.[13−27] Sum frequency generation studies of water uptake on mica suggest a monolayer of icelike water when the RH is near 90%;[14] however, these data are in conflict with both ellipsometry and expected film thicknesses for a type II adsorption isotherm on highly hydrophilic surfaces.[15] These studies have not fully elucidated the structural evolution of the water molecule configuration, as water molecules are adsorbed on the silicon oxide surface under ambient conditions directly relevant to atmospheric phenomena, material behavior, and device operations.

* Corresponding author. E-mail: shkim@engr.psu.edu.

In this study, the structure of adsorbed water on a silicon oxide surface was investigated with attenuated total reflection−infrared (ATR−IR) spectroscopy.[28] A silicon ATR crystal covered with a native oxide was used. In this analysis, the probe IR beam travels inside the solid silicon substrate and is totally reflected at the substrate surface. A shallow evanescent wave penetrates into the adsorbed layer and the gas phase. However, the gas-phase molecules are not detected due to the low molecular density. Even at the saturated vapor pressure of water at room temperature, the number of gas-phase molecules present in the probe volume above the 1 cm^2 ATR crystal surface is $\sim 3 \times 10^{13}$, or less than 4% of a single-layer molecular density. Therefore, only the adsorbed molecules are detected, enabling a vibrational spectroscopic study for identification of the molecular configuration of water in the adsorbed layer without interference from the gas-phase water molecules. The ATR−IR natural log of the reflectance is proportional to the distribution of different configurations as well as the total thickness of the adsorbed water layers.[28]

The data presented in this paper reveal the structural profile of the adsorbed water layers as they grow thicker with relative humidity. The first three layers adsorbed on the silicon oxide surface at low humidities conform to an "icelike" configuration; the next layer formed in medium humidities is in a transition between the completely self-associated network and a liquidlike configuration; and finally, the subsequently adsorbed water layers at high humidities assume the bulk liquid configuration. The evolution of these structures indicates that transitions in equilibrium at the interface influence the shape of the adsorption isotherm curve. The structural changes of the outermost water layer of the interface due to these transitions illuminate lingering questions regarding adhesion, protein adsorption, water structure at interfaces, and wetting.

Experimental Details

ATR spectra were collected using a Thermo-Nicolet Nexus 670 spectrometer with a MCT detector and a multiple-bounce

10.1021/jp053042o CCC: $30.25
Published on Web 08/13/2005

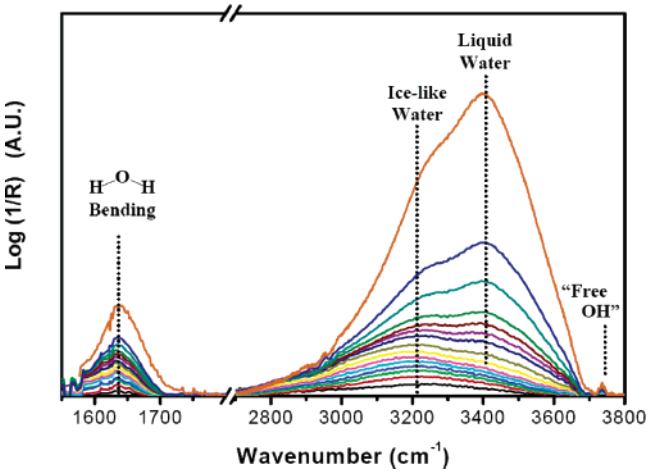

Figure 1. ATR−IR spectra of water adsorbed on silicon oxide at different relative humidities. From lowest to highest log (1/*R*) signal intensity, relative humidity = 7.3, 9.7, 14.5, 19.4, 24.5, 29.4, 38.8, 49.4, 58.6, 64.3, 69.9, 74.5, 84.2, 92.2, and 99.4%. The O−H stretching vibration peak positions of "icelike" water and liquid water are marked with dotted lines at ~3230 and ~3400 cm^{-1}, respectively. The free-OH peak is marked at 3740 cm^{-1}.

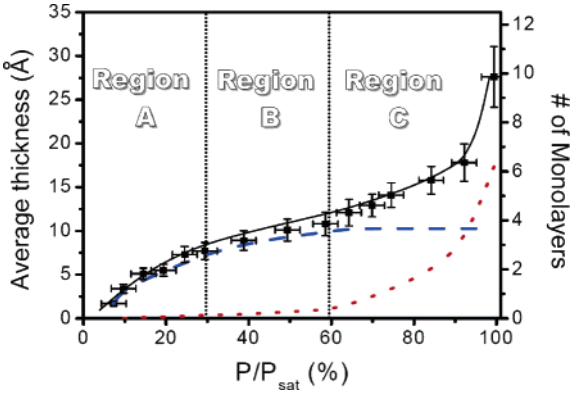

Figure 2. Adsorption isotherm of adsorbed water on the silicon oxide surface. Square symbols are the total thickness of the adsorbed water layer calculated from the intensity of the H−O−H bending vibration peak. The solid line is drawn to guide eyes. The dashed and dotted lines are the thickness of the icelike water and liquid water layers, respectively. The thickness of each component is calculated by deconvoluting the observed O−H stretching peaks into two peaks at 3230 and 3400 cm^{-1}. The sensitivity of the O−H stretching peak is assumed to be equal in both structures. Regions A, B, and C are shown, corresponding to icelike water growth, transitional growth, and liquid water growth (see text for details).

silicon ATR crystal. The crystal was prepared by washing with dichloromethane, rinsing with copious amounts of Millipore water, drying with argon, and exposing it to UV/O_3 for 30 min. This procedure produced an organic-contaminant-free native oxide surface believed to be saturated with hydroxyl groups.[29] Following the cleaning, the silicon crystal was promptly mounted to the ATR assembly and purged with dry Ar until there was no change in background spectra. The adsorption of water onto this surface was accomplished by varying the ratio of dry argon flow to water-saturated argon stream. The temperature of the system was maintained at 20.8 ± 0.5 °C, while the partial pressure of water was varied from 0 to 100%. At an incident angle of 45°, the effective penetration depth of the evanescent wave was 482 nm at 1635 cm^{-1}. The molar absorptivities of the H−O−H bending region of ice and liquid water estimated from refs 19, 30, 31 differ by less than 20%.

Results and Discussion

Figure 1 contains the ATR−IR spectra of the adsorbed water layers on the silicon oxide surface as a function of relative humidity. There are two absorption bands: a single peak at 1640 cm^{-1} due to the H−O−H bending vibration and a group of peaks in the 3000−3800 cm^{-1} region due to the O−H stretching vibrations.[32] Because the bending vibration at 1640 cm^{-1} does not vary significantly with the configuration of water molecules in the adsorbed layer, its intensity is used to determine the average thickness of the adsorbed layer. The thickness is determined by comparing the IR absorption due to the adsorbed water molecules with the IR absorption of bulk water on the ATR crystal. The adsorption isotherm thickness determined from the intensity of the 1640 cm^{-1} peak is plotted in Figure 2. The monolayer thickness is calculated by dividing the measured thickness by 2.82 Å, the mean van der Waals diameter of water. If the bilayer thickness (4 Å) is used, the number of water layers would be slightly larger. Details of the short-range ordering on native oxides are unknown at this time. The average thickness determined from the ATR intensity follows the typical type II isotherm curve of water. The data are in good agreement with previously reported data for hydrophilic surfaces.[13,15]

In the O−H stretching vibration region, there are three peaks of interest: a small sharp peak at 3740 cm^{-1} and two broad peaks at 3230 and 3400 cm^{-1}. The peak at 3740 cm^{-1} seems to be due to "free OH" or a hydroxyl group with no hydrogen bonds.[32,33] This peak appears because the outermost adsorbed water molecules do not have sufficient nearest neighbors to saturate hydrogen bonding. The silicon oxide surface is initially saturated with surface OH groups (those bonded to Si). The single beam spectrum of this surface was used as a background. As water adsorbs on this surface, the surface/air interface eventually becomes saturated with water OH groups. The presence of the 3740 cm^{-1} peak in the background-subtracted spectra may suggest a slight difference in free OH environments between the solid/dry air interface and the water/air interface.[34]

Detailed information regarding the molecular configuration of water in the adsorbed layer can be found from analysis of the two peaks at 3230 and 3400 cm^{-1} corresponding to the stretching vibrations of completely self-associated "icelike" water and "liquid" water, respectively.[19,22,32] As the degree of hydrogen bonding increases, the O−H stretching vibration shifts to lower wavenumbers. As water is initially introduced in the gas phase, the icelike water peak at 3230 cm^{-1} grows exclusively up to a relative humidity (RH) of ~30%. The liquid water peak at 3400 cm^{-1} starts growing along with the icelike water peak as the RH increases up to ~60%. At a RH of 65−70%, the apparent peak intensities of these two peaks appear the same. With further increase of RH, the liquid water peak at 3400 cm^{-1} becomes dominant. It should be noted that the evolution of these two peaks does not originate from distortion of the ATR−IR band due to the nonlinear variation of the refractive index with wavelength near absorption bands and strong attenuation index of water.[35] In the case of ATR measurements of bulk water, we observed a shift of the O−H stretching vibration peak position to a lower wavenumber (3370 cm^{-1}) due to the abnormal dispersion effects; however, this kind of red-shift is not observed at all for the adsorbed water molecules. These results clearly reveal that the molecular configuration of water changes as the adsorbed layer thickness increases.

The relative abundance of the icelike and liquid water is determined by deconvolution of the IR spectra in the 2800−3700 cm^{-1} region into the 3230 and 3400 cm^{-1} peaks. The result of this analysis is plotted in Figure 2, along with the total thickness of the adsorbed water layer calculated from the

H−O−H bending vibration peak. At RH below 30% (marked as region A), the icelike structure grows up to ~3 molecular layers. The total thickness increases rapidly at the beginning; then its growth rate slows. In the RH range of 30−60% (marked as region B), the liquid structure starts growing slowly, although the icelike structure is still dominant. In this region, the total thickness increases linearly with RH from 3 to 4 monolayers. At RH above 60% (marked as region C), the icelike structure growth ends and only the liquid structure grows rapidly with increase of RH. In the following paragraphs, we discuss the origin of different structures and growth patterns for each region.

In region A, the adsorption isotherm thickness increases rapidly and then retards, giving a "kneelike" shape. In the case of many organic molecules, this shape is attributed to completion of the one monolayer adsorption. Once the monolayer is formed, the thickness does not grow until the relative partial pressure approaches saturation.[36] In the case of water, the initial rise does not stop at the completion of a monolayer; instead, it continues growing up to three layers. This is due to the hydrogen bonding capacity of the water molecule. Formation of hydrogen bonds with the immobilized substrate hydroxyl groups forces water molecules in the first layer into an ordered structure. The induced structure of the first layer propagates through hydrogen bonds into upper layers. This is possible because water can form a tetrahedrally coordinated icelike network. In this region, the interface can be considered in equilibrium between the surface-induced icelike layer and water vapor, a pseudo-solid (ice)−vapor equilibrium.

In region B, the surface-induced structuring effect at the outermost adsorbed layer starts diminishing. We consider the growth in this region to be in transition between the two water structure growths. The structural rigidity of the hydrogen bonding network competes with thermal motions of the adsorbing water molecules at room temperature; the liquid water structure starts appearing at RH ~30%. In other words, the growth of the liquidlike layer begins before the growth of the icelike water layer ends. However, the liquid water structure is not yet fully stable and does not form multilayers because the relative humidity in the gas phase is not high enough. This is the reason that the growth rate of water in this region is small, accounting for only one molecular layer increase over RH increase from 30 to 60%. These transitions cause the change in curvature of the Type II isotherm. The fact that growth of the icelike structure is still dominating until it saturates at RH ~60% indicates that these molecules are still under a strong influence of the immobilized surface hydroxyl groups.

As the relative humidity increases above ~60%, the structure of the outermost layer is completely dominated by thermal motion so it assumes a liquid water configuration. The thickness of the adsorbed layer starts increasing exponentially with RH, and bulk condensation occurs at near saturation vapor pressure. In region C, the outermost adsorbed layer is in equilibrium between the liquid water layer and vapor.

Figure 3 summarizes the evolution of two distinct structures as water adsorbs on silicon oxide. The first three layers, those closest to the immobilized hydroxyl surface (Si−OH), form an icelike network. Above the icelike water, there exists a transitional region whose structure is more relaxed than the underlayers of the icelike structure, but not completely disordered as are the liquid layers above it. Any additional water adsorbing on this surface behaves as a liquid. This structural evolution indicates changes in the nature of the interfacial equilibrium at different humidity regions and coincides with the smooth transitions of the adsorption isotherm curve.

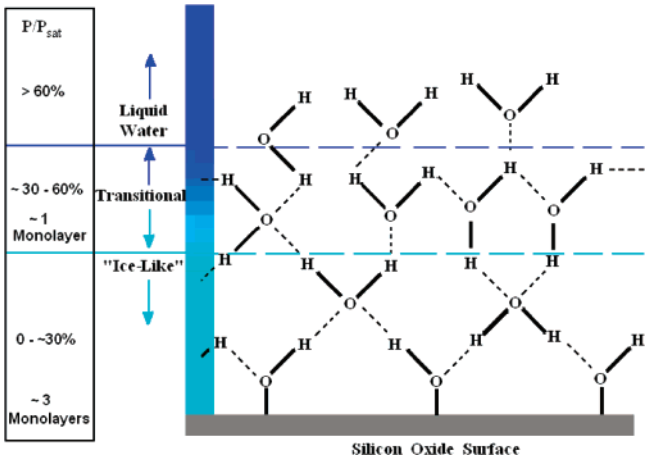

Figure 3. Schematic illustrating the structural evolution of water molecules as the adsorbed layer thickness increases with RH. The icelike structure grows up to 3 molecular layers thick as relative humidity increases from 0 to 30%. In the relative humidity range from 30 to 60%, the icelike structure continues to grow while liquid structure begins to form. In this transitional RH region, approximately one molecular layer grows. Further increase in the relative humidity above 60% causes water to adsorb in the liquid configuration (--- hydrogen bonds, — covalent bonds). (Note: 2-D illustration is not to scale).

The formation of an icelike structure at low humidities is consistent with what have been implicated from other spectroscopic observations. In nuclear magnetic resonance spectroscopy studies, the adsorbed water molecules exhibit two different relaxation times—one is close to that of bulk water, and the other is much slower.[24] This slow relaxation time phase must be related to the "icelike" water structure. As a matter of fact, the slow relaxation time phase is reported to be dominant at low humidity. Dielectric measurements of the adsorbed water on hydroxylated chromium oxide at room temperature also found that the relaxation time of the adsorbed water is several orders of magnitude lower than that of bulk water.[37]

The implications of structured water at the silicon oxide interface in nature are many. The structure of the adsorbed water layer at the interface of silicon oxide and humid gas (Figure 3) provides insight into many phenomena observed for silicon oxide surfaces in humid environments. The hardening of cement upon drying would be an example that can be explained in part with our structural model.[10] As the cement dries, contacts between hydrophilic silica particles form icelike bridges that are stronger than the liquid. Another example is the nanoscale contact mechanics of clean silicon oxide surfaces. The adhesion force of silicon oxide surfaces measured with atomic force microscopy increases as the humidity increases, reaches a maximum value at an intermediate humidity, and then finally decreases as the humidity approaches the saturation vapor pressure of water.[8,9] This kind of complicated adhesive behavior of nanoscale contacts is witnessed only with water. There have been many attempts to predict this complicated behavior with a simple capillary condensation theory using the Kelvin equation and the surface tension of bulk water (72 erg/cm^2); however, the estimated magnitude of the adhesion force change is much smaller than what is observed experimentally.[9] Our ATR−IR data and the model indicate that the surface tension value of bulk water cannot be used at RH < 60% because the adsorbed water molecules are in the icelike configuration.

The surface tension of the icelike layer may be estimated from the following calculation. The average hydrogen bond number of liquid water is about 2.5 per molecule, while that of ice is 4 per molecule.[38] The Fowkes theory predicts that the

van der Waals contribution to the water surface tension is ~23 erg/cm^2.[39] The remaining ~50 erg/cm^2 can be attributed to 2.5 hydrogen bonds in liquid water. From this first-order approximation, the surface tension contribution for 4 hydrogen bonds is expected to be ~80 erg/cm^2. Therefore, the surface tension of the adsorbed water layer at RH below 60% will be ~103 erg/cm^2, which is close to the surface tension of ice.[40,41] This is one reason that adhesion between silicon oxide surfaces at low RH is higher than that at high RH.[8,9,42] More details are the subject of a separate paper.[42]

Although the structure shown in Figure 3 is determined during the equilibrium adsorption from the gas phase, the entire structure can be applied to the silicon oxide and bulk water interface.[16,19,23] The structure and thickness of the bottom "icelike" layer do not change with the thickness of the liquid-structure overlayer. The presence of these icelike layers on hydrophilic silicon oxide surfaces can, in part, account for lower bio-fouling activity on these surfaces compared to hydrophobic surfaces. At hydrophobic surfaces, water is not strongly bound with the surface so it is easy for biomolecules such as proteins to displace the water and occupy space at the surface. At hydrophilic surfaces, the cohesive hydrogen bonding within the icelike network is so strong and thick that protein molecules cannot easily replace the water molecules in this icelike network.[1,5] Another interesting and important phenomenon is the nucleation kinetics of ice. It has recently been found that nucleation of ice occurs much faster on quartz surfaces than on alumina surfaces.[43] Since the preferential formation of the icelike structure on alumina is not observed,[21] these results may indicate that the icelike layer on quartz acts as a seed for the nucleation of ice.

Conclusions

This study elucidates how hydrogen bonding with immobilized surface hydroxyl groups (Si−OH) affects the molecular configuration of the adsorbed water at ambient conditions. The equilibrium structure of the outermost layer varies in three different regions of the adsorption isotherm. In low humidity (RH below 30%), the adsorbed water forms an icelike network on the silicon oxide surface that propagates up to ~3 layers from the surface at room temperature. The hydrogen bond network structure competes with the liquid water structure in the RH range of 30−60%, above which the liquid structure dominates. These structural transitions have profound effects on the adsorption isotherm of water and the behavior of the silicon oxide surface in different environments.

Acknowledgment. This work is financially supported by the National Science Foundation (Grant No. CMS-048369).

References and Notes

(1) Vogler, E. A. *Adv. Colloid Interface Sci.* **1998**, *74*, 69.
(2) Pruppacher, H. R.; Klett, J. D. *Microphysics of Clouds and Precipitation*; Kluwer Academic Publishers: The Netherlands, 1997.
(3) Stumm, W.; Sigg, L.; Sulzberger, B. *Chemistry of the Solid-Water Interface*: *Processes at the Mineral-Water and Particle-Water Interface in Natural Systems*; Wiley: New York, 1992.
(4) de Gennes, P. G. *Rev. Mod. Phys.* **1985**, *57*, 827.
(5) Margel, S.; Vogler, E. A.; Firment, L.; Watt, T.; Haynie, S.; Sogah, D. Y. *J. Biomed. Mater. Res.* **1993**, *27*, 1463.
(6) Maboudian, R.; Howe, R. T. *J. Vac. Sci. Technol. B* **1997**, *15*, 1.
(7) Urbakh, M.; Klafter, J.; Gourdon, D.; Israelachvili, J. *Nature* **2004**, *430*, 525.
(8) Binggeli, M.; Mate, C. M. *Appl. Phys. Lett.* **1994**, *65*, 415.
(9) Xiao, X.; Qian, L. *Langmuir* **2000**, *16*, 8153.
(10) Taylor, H. F. *Cement Chemistry*, 2nd ed.; Academic Press: London, 1997.
(11) Stevenson, K. P.; Kimmel, G. A.; Dohnalek, Z.; Smith, R. S.; Kay, B. D. *Science* **1999**, *283*, 1505.
(12) Henderson, M. A. *Surf. Sci. Rep.* **2002**, *46*, 1.
(13) Thiel, P. A.; Madey, T. E. *Surf. Sci. Rep.* **1987**, *7*, 211.
(14) Miranda, P. B.; Xu, L.; Shen, Y. R.; Salmeron, M. *Phys. Rev. Lett.* **1998**, *81*, 5876.
(15) Beaglehole, D.; Christenson, H. K. *J. Phys. Chem.* **1992**, *96*, 3395.
(16) Hasegawa, T.; Nishijo, J.; Imae, T.; Huo, Q.; Leblanc, R. M. *J. Phys. Chem. B* **2001**, *105*, 12056.
(17) Scatena, L. F.; Brown, M. G.; Richmond, G. L. *Science* **2001**, *292*, 908.
(18) Yalamanchili, M. R.; Atia, A. A.; Miller, J. D. *Langmuir* **1996**, *12*, 4176.
(19) Ewing, G. E. *J. Phys. Chem. B* **2004**, *108*, 15953.
(20) Trakhtenberg, S.; Naaman, R.; Cohen, S. R.; Benjamin, I. *J. Phys. Chem. B* **1997**, *101*, 5172.
(21) Al-Abadleh, H. A.; Grassian, V. H. *Langmuir* **2003**, *19*, 341.
(22) Du, Q.; Freysz, E.; Shen, Y. R. *Science* **1994**, *264*, 826.
(23) Toney, M. F.; Howard, J. N.; Richer, J.; Borges, G. L.; Gordon, J. G.; Melroy, O. R.; Wiesler, D. G.; Yee, D.; Sorensen, L. B. *Surf. Sci.* **1995**, *335*, 326.
(24) Zimmerman, J. R.; Lasater, J. A. *J. Phys. Chem.* **1958**, *62*, 1157.
(25) D'Orazio, F.; Bhattacharja, S.; Halperin, W. P.; Eguchi, K.; Mizusaki, T. *Phys. Rev. B* **1990**, *42*, 9810.
(26) Hu, J.; Xiao, X.-D.; Ogletree, D. F.; Salmeron, M. *Science* **1995**, *268*, 267.
(27) Yang, J.; Meng, S.; Xu, L.; Wang, E. G. *Phys. Rev. B* **2005**, *71*, 035413.
(28) Urban, M. W. *Attenuated Total Reflectance Spectroscopy of Polymers Theory and Practice*; American Chemical Society: Washington, DC, 1996.
(29) Graubner, V.-M.; Jordan, R.; Nuyken, O.; Schnyder, B.; Lippert, T.; Kotz, R.; Wokaun, A. *Macromolecules* **2004**, *37*, 5936.
(30) Warren, S. G. *Appl. Opt.* **1984**, *23*, 1206.
(31) Venyaminov, S. Y.; Prendergast, F. G. *Anal. Biochem*. **1997**, *248*, 234.
(32) Scherer, J. R. *Advances in Infrared and Raman Spectroscopy*; Heyden: London, 1978; Vol. 5.
(33) Ratcliffe, C. I.; Irish, D. E. *J. Phys. Chem*. **1982**, *86*, 4897.
(34) Zhuravlev, L. T. *Langmuir* **1987**, *3*, 316.
(35) Hancer, M.; Sperline, R. P.; Miller, J. D. *Appl. Spectrosc.* **2000**, *54*, 138.
(36) Adamson, A. W.; Gast, A. P. *Physical Chemistry of Surface*, 6th ed.; John Wiley & Sons: New York, 1997.
(37) Kuroda, Y.; Kittaka, S.; Takahara, S.; Yamaguchi, T.; Bellissent-Funel, M.-C. *J. Phys. Chem. B* **1999**, *103*, 11064.
(38) Weber, T. A.; Stillinger, F. H. *J. Phys. Chem.* **1983**, *87*, 4277.
(39) Fowkes, F. M. *J. Phys. Chem.* **1963**, *67*, 2538.
(40) Douillard, J. M.; Henry, M. *J. Colloid Interface Sci.* **2003**, *263*, 554.
(41) Jang, J.; Schatz, G. C.; Ratner, M. A. *Phys. Rev. Lett.* **2004**, *92*, 085504.
(42) Asay, D. B.; Kim, S. H. To be submitted.
(43) Dolan, D. H.; Gupta, Y. M. *J. Chem. Phys.* **2004**, *121*, 9050.